Effect of Thermal Properties of a Coated Elastohydrodynamic Lubrication Line Contact Under Various Slide-to-Roll Ratios

Huaiju Liu
State Key Laboratory of Mechanical Transmissions,
Chongqing University,
Shazhengjie 174,
Chongqing 400044, China
e-mail: huaijuliu@cqu.edu.cn

Caichao Zhu
State Key Laboratory of Mechanical Transmissions,
Chongqing University,
Shazhengjie 174,
Chongqing 400044, China
e-mail: cczhu@cqu.edu.cn

Zonglin Gu
State Key Laboratory of Mechanical Transmissions,
Chongqing University,
Shazhengjie 174,
Chongqing 400044, China
e-mail: 1148752323@qq.com

Zhanjiang Wang
Department of Mechanical Engineering,
Southwest Jiaotong University,
Chengdu 610031, China
e-mail: wangzhanjiang001@gmail.com

Jinyuan Tang
State Key Laboratory of High Performance
Complex Manufacturing,
Central South University,
Changsha 410083, Hunan, China
e-mail: jytangcsu@163.com

A numerical thermal elastohydrodynamic lubrication (EHL) model is developed for coated line contacts by considering both the mechanical properties and the thermal properties of the coating and the substrate. The temperature fields within the oil film and within the solids are solved by deriving the energy equations for the solids and the oil film. Heat continuity conditions are satisfied at the interfaces between the solids and the oil film, and the coating/substrate interfaces. Effects of the slide-to-roll ratio (SR), the thermal conductivities of the coating bodies, and the oil film on temperature fields are studied. [DOI: 10.1115/1.4036078]

Introduction

Coatings are extensively applied in engineering, such as surfaces of gear tooth, cams and bearings, etc., due to their good tribological performance [1–4]. The usage of coating on engineering surfaces aims at either the reduction of the friction and wear or the improvement of surface durability. Theoretical studies on the tribological effect of coatings started from the cases of rigid substrates bonded to elastic coatings such as those shown in Refs. [5,6]. Recently, the frequency response functions, relating the contact pressure to the surface displacement and stress components, derived from the Papkovich–Neuber potentials, have been used for the calculation of multilayer contact problems by Wang et al. [7]. However, most coated contact studies assumed the isothermal condition and attentions were mainly paid to the effects of the rigidity and the thickness of the coating on the pressure and the film thickness during contacts [8]. Under a lubricated sliding-while-rolling condition with heavy normal load, the shear stress within the oil film, due to the relative motion between the two interacting surfaces, causes significant temperature rise within the contact area. The temperature rise changes the viscosity and the shear stress of the lubrication film, which further affects the frictional behavior and the surface failure behavior such as scuffing. Björling et al. [9] concluded that the significantly reduced friction in the diamond-like carbon (DLC)-coated EHL contact was mainly due to the thermal phenomenon. The consideration of the thermal effect in a lubricated contact problem leads to the coupling of the temperature field and the pressure field within the contact zone and a thermo-lubrication model is often required. Yang et al. [10] developed a thermo-elastohydrodynamic lubrication (TEHL) model to solve contact problems. However, most thermal lubrication models are limited to uncoated contact cases.

Generally, the coating and the substrate materials differ not only in the mechanical properties such as the Young's modulus and the Poisson's ratio but also in the thermal properties such as the heat capacity and the thermal conductivity. The thermal conductivity of the steel frequently used as the substrate material in engineering is approximately 30–50 W/(m K), while Liu et al. [11] suggested that the thermal conductivity of the DLC coatings was in the range of 0.7–7 W/(m K) depending on the film composition and the structure. In a general contact problem, the differences in the thermal properties between the coating, the substrate and the oil film affect the tribological performance which is yet to be discovered. This work studies the effects of the thermal properties of the solids and the oil film such as the thermal conductivity and the heat capacity on the tribological performance of a coated EHL line contact by developing a numerical thermal-elastohydrodynamic lubrication model which considers the differences in the mechanical and thermal properties between the coating and the substrate. The energy equations of the oil film, the coating, and the substrate are derived, respectively. The generalized Reynolds equation, first proposed by Yang and Wen [12], is applied to incorporate the effect of the Ree-Eyring non-Newtonian fluid behavior and the thermal effect on the pressure distribution. The two-dimensional frequency response function derived in Ref. [13], relating the pressure to the surface displacement, is utilized in combination with the discrete convolute, fast Fourier transform (DC-FFT) method [14] to incorporate the effect of mechanical properties of the coating.

Methodology

The lubricated line contact between two smooth coated rollers is studied, which is a suitable simplification of many engineering applications such as the contact of the spur gear tooth or the roller bearing. It is easy to further incorporate the surface roughness in the model; however, the roughness is ignored in this current work. The two coated rollers (solids a and b) are rolling with their own rolling velocities under an external normal load F (unit N/m), as shown in Fig. 1. The thermal properties as well as the mechanical properties of the substrates, the coatings, and the oil film are listed in the figure.

The governing energy equations for the oil film and the solids are different from each other, and therefore along the z direction, representing the direction of the normal load, the film and the solids are treated separately, as shown in Ref. [15]. The energy equation of the oil film can be expressed as

Contributed by the Heat Transfer Division of ASME for publication in the Journal of Heat Transfer. Manuscript received April 28, 2016; final manuscript received January 24, 2017; published online April 4, 2017. Assoc. Editor: Ali Khounsary.

 Copyright © 2017 by ASME

Downloaded From: https://heattransfer.asmedigitalcollection.asme.org/pdfaccess.ashx?url=/data/journals/jhtrao/936122/ on 04/16/2017 Terms of Use: http://www.asme.org/abou

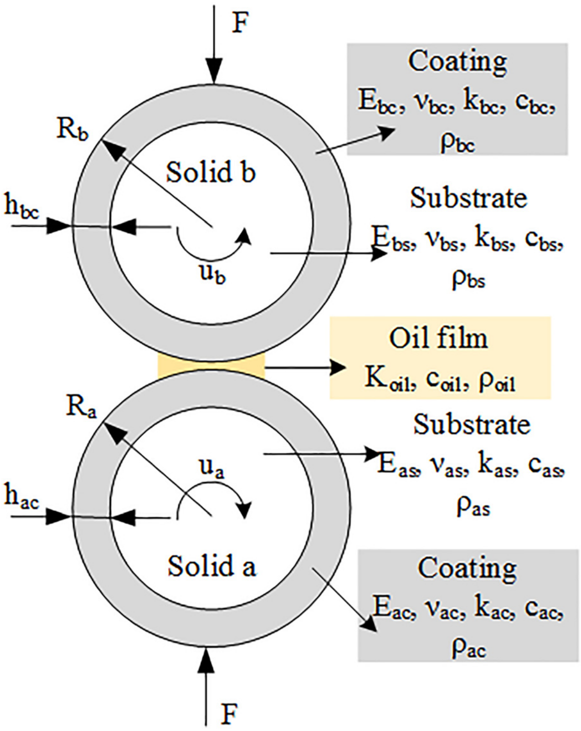

Fig. 1 The lubricated contact between two coated rollers

$$\underbrace{c_{\text{oil}}\left[\rho_{\text{oil}}u\frac{\partial T}{\partial x}-\frac{\partial}{\partial x}\int_0^z\rho_{\text{oil}}u dz'\frac{\partial T}{\partial z}\right]}_{\text{Heat convection}}+\underbrace{\frac{T}{\rho_{\text{oil}}}\frac{\partial\rho_{\text{oil}}}{\partial T}\frac{u\partial p}{\partial x}}_{\text{Compression heat}}$$

$$=\underbrace{k_{\text{oil}}\frac{\partial^2 T}{\partial z^2}}_{\text{Heat conduction}}+\underbrace{\eta_{\text{oil}}\left(\frac{\partial u}{\partial z}\right)^2}_{\text{Viscous heat}} \quad (1)$$

where c_{oil}, ρ_{oil}, and k_{oil} are the heat capacity (unit J/(kg K)), the density (unit kg/m^3), and the thermal conductivity (unit W/m K) of the fluid, respectively. T is the temperature with unit K and u is the velocity along the rolling direction (x-direction) of the fluid (unit m/s).

The energy equations within the two solids are [16]

$$\begin{cases} c_{aj}\rho_{aj}u_a\dfrac{\partial T}{\partial x}=k_{aj}\dfrac{\partial^2 T}{\partial z_a^2} \;\; (j=c,s) \\ c_{bj}\rho_{bj}u_b\dfrac{\partial T}{\partial x}=k_{bj}\dfrac{\partial^2 T}{\partial z_b^2} \;\; (j=c,s) \end{cases} \quad (2)$$

where c_{ij}, ρ_{ij}, $k_{ij}(i=a,b;j=c,s)$ are the heat capacity (unit J/kg K), the density (unit kg/m^3), and the thermal conductivity (unit W/m K) of the coating and the substrate of solid a and solid b, respectively. $z_i(i=a,b)$ represents the depth inside each solid.

The solid and the oil film should have the same temperature at their interface. This heat flux continuity condition reads

$$\begin{cases} k_{\text{oil}}\dfrac{\partial T}{\partial z_{\text{oil}}}\Big|_{z_{\text{oil}}=0}=k_{ac}\dfrac{\partial T}{\partial z_a}\Big|_{z_a=0} \\ k_{\text{oil}}\dfrac{\partial T}{\partial z_{\text{oil}}}\Big|_{z_{\text{oil}}=h}=k_{bc}\dfrac{\partial T}{\partial z_b}\Big|_{z_b=0} \end{cases} \quad (3)$$

The heat continuity equations at the coating/substrate interfaces of the solids are expressed as

$$\begin{cases} k_{ac}\dfrac{\partial T}{\partial z_a}\Big|_{z_a=h_{ac}}=k_{as}\dfrac{\partial T}{\partial z_a}\Big|_{z_a=h_{ac}} \\ k_{bc}\dfrac{\partial T}{\partial z_b}\Big|_{z_b=h_{bc}}=k_{bs}\dfrac{\partial T}{\partial z_b}\Big|_{z_b=h_{bc}} \end{cases} \quad (4)$$

where $h_{ic}(i=a,b)$ represents the thickness of the coating of each solid.

The boundary conditions of the temperature field can be expressed as

$$\begin{cases} T(x_{\text{in}},z_{\text{oil}})=T_0\,(\text{when } u(0,z_{\text{oil}})\geq 0,\ z_{\text{oil}}\in[0,h]) \\ T(x_{\text{in}},z_a)=T_0\,(z_a\in[-d,0]) \\ T(x_{\text{in}},z_b)=T_0\,(z_b\in[0,d]) \\ T(x,d)=T(x,-d)=T_0\,(x\in[x_{\text{in}},x_{\text{out}}]) \end{cases} \quad (5)$$

In this work, the boundary d is chosen as $d=2b_h$.

The generalized Reynolds equation, considering the variation of the velocity of the fluid across the film thickness, is applied and detailed expression can be found in Ref. [17]. The elastic deformation is calculated using the DC-FFT method with the influence coefficient obtained through the frequency response function, which relates the pressure to the surface displacement [18]. The Roelands viscosity–pressure–temperature relation [19] and the Dowson and Higginson density–pressure relation [20] are applied to describe the viscosity and the density of the fluid, respectively.

The dimensionless form and the discretization scheme are available in Ref. [15]. The coefficient matrix of the set of governing equations of the temperature field can be written as a tridiagonal matrix which is diagonally dominant. This set of equations can be solved efficiently with the chasing method. In this work, 1025 equally spaced nodes are arranged along the rolling direction within the calculation domain $X_i\in[-4,3]$ ($\mathrm{i}=0,1,...,1024$). The convergence criteria of the pressure P, the normal load $\sum|P_i|\Delta X$, and the temperature T at any transient time step are chosen as $\sum|P_i-P_i'|/\sum|P_i|<0.00001$, $|\sum|P_i|\Delta X-(\pi/2)|/(\pi/2)<0.0001$, and $\sum\sum|\overline{T_{i,k}}-\overline{T'_{i,k}}|/\sum\sum|\overline{T_{i,k}}|<0.00001$, respectively, where P_i is the updated dimensionless pressure and P_i' is the old dimensionless pressure value, $\overline{T_{i,k}}$ is the updated dimensionless temperature and $\overline{T'_{i,k}}$ is the old dimensionless temperature before the current iteration.

Results and Discussion

The working conditions and properties of the lubricant and the solids are listed in Table 1. The mechanical properties of the substrate materials of solids a and b are kept the same. The coating thickness of solids a and b is identical with each other. A large range of the slide-to-roll ratio $\mathrm{SR}\in[0.1,2.0]$ is selected to represent common conditions occurring in engineering applications such as gear drives. The thermal properties such as the thermal conductivity, the heat capacity of the solids, and of the oil are manually changed within a large range to show their effects on the tribological performance of the lubricated contact.

The effect of mechanical properties, i.e., the rigidity and the thickness of the coating, on the pressure and the film thickness has already been studied in Refs. [21–23]. The current model is validated through the comparison of the pressure profile and the film thickness with previous results.

The slide-to-roll ratio is an important parameter affecting the tribological behavior of the contact bodies. Not only the surface failure mechanism is affected but also the friction and the temperature rise are influenced by the slide-to-roll ratio significantly. Figure 2 shows the effect of slide-to-roll ratio on the temperature profile at five characteristic layers along the normal load direction, i.e., the coating/substrate (C/S) interfaces and the surfaces of the two solids and the central oil film layer, under the working condition $F=5\times10^5$ N/m, $u_r=1$ m/s, $E_c=2E_s$, $h_c=100\,\mu$m,

Downloaded From: https://heattransfer.asmedigitalcollection.asme.org/pdfaccess.ashx?url=/data/journals/jhtrao/936122/ on 04/16/2017 Terms of Use: http://www.asme.org/abou

Table 1 Working conditions and properties of the lubricant and the solids

Normal load, F	$F = 5 \times 10^5$ N/m	Thermal conductivity of the oil k_{oil}	$k_{oil} = (0.07–0.65)$ W/m K
Rolling speed, u_r	$u_r = 1.0$ m/s	Thermal conductivity of the substrate material k_s	$k_s = 46$ W/m K
Slide-to-roll ratio, SR	SR = 0.1–2.0	Thermal conductivity of the coating material k_c	$k_c = (0.125–4)k_s$
Radius of curvature, R_a, R_b	$R_a = R_b = 0.05$ m	Heat capacity of the oil c_{oil}	$c_{oil} = 2000$ J/kg K
Young's modulus of the substrate, E_s	$E_s = 2.0 \times 10^{11}$ Pa	Heat capacity of the substrate material c_s	$c_s = 470$ J/kg K
Young's modulus of the coating, E_c	$E_c = (0.25–4.5)E_s$	Heat capacity of the coating material c_c	$c_c = c_s$
Poission's ratio of materials, ν	$\nu = 0.3$	Ambient density of the lubricant ρ_{oil0}	$\rho_{oil0} = 870$ kg/m^3
Coating thickness, h_{ca}, h_{cb}	$h_{ac} = h_{bc} = 100$ μm	Density of the substrate and the coating ρ_c, ρ_s	$\rho_c = \rho_s = 7850$ kg/m^3
Eyring stress, τ_0	$\tau_0 = 10$ MPa	Ambient temperature and the inlet oil temperature T_0	$T_0 = 313$ K
The pressure–viscosity coefficient	$\alpha = 2.2 \times 10^{-8}$ Pa^{-1}	Oil viscosity at ambient pressure	$\eta_{oil0} = 0.04$ Pa · s

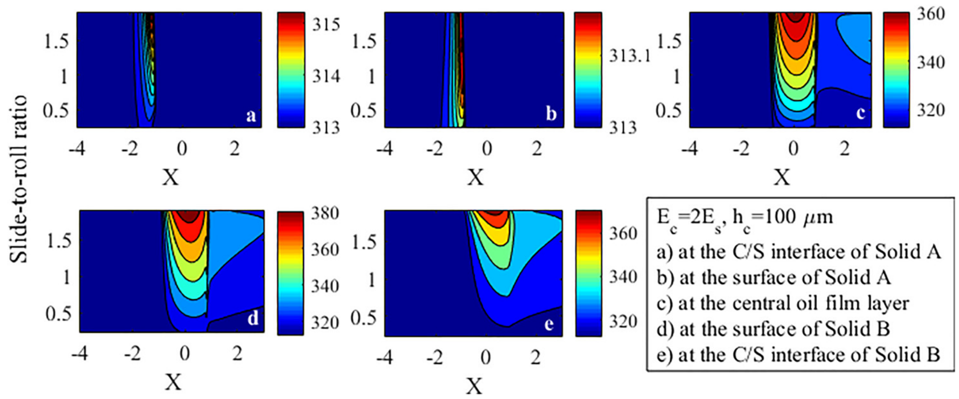

Fig. 2 Effect of slide-to-roll ratio on temperature profile at five characteristic layers

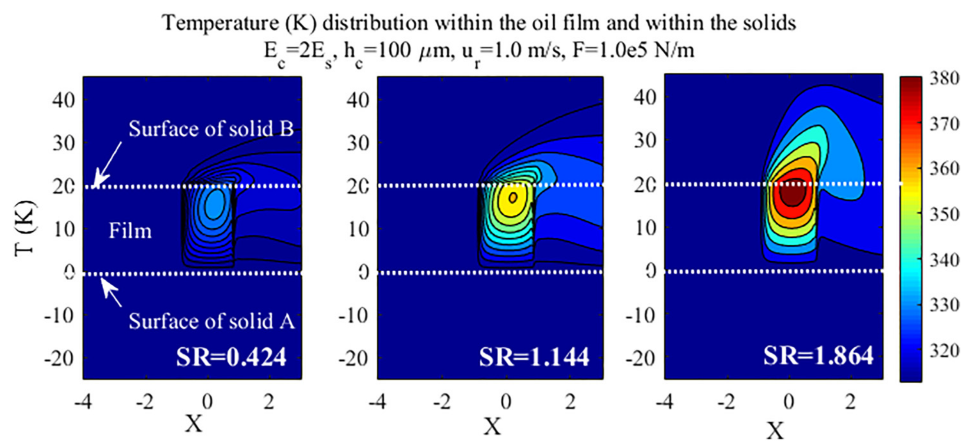

Fig. 3 The temperature distribution under three slide-to-roll ratio cases

$k_{ca} = k_{cb} = k_s$, and $c_{ca} = c_{cb} = c_s$. When the slide-to-roll ratio changes, the temperature at each layer varies consequently. The variations at the central oil film layer, the surface of solid b and its C/S interface are significant, while those at the surface of solid a and its C/S interface are negligible. Difference of the temperature distribution within the two solids is caused by their difference in the rolling speed, and in this case, $u_a > u_b$. The maximum temperature rise goes up with the increasing slide-to-roll ratio. The temperature rise mainly occurs within the Hertzian contact zone. The temperature of the surface with the smaller rolling velocity is higher than that of the surface with the larger rolling velocity. But when the sliding velocity is no longer negligible, the temperature rise at the C/S interface of the solid with the smaller rolling velocity is significant.

Figure 3 shows the whole temperature field within the oil film and the solids under three slide-to-roll ratios, i.e., SR = 0.424, 1.144, 1.864. It shows clearly that the temperature rise inside the oil film increases significantly as the slide-to-roll ratio increases. The maximum temperature rise increases from 5% for the case SR = 0.424 to 21% for the case SR = 1.864. Under the latter case, the highest temperature within the contact reaches 380 K. Since there is a sliding velocity between the surfaces of the two solids, the location of the maximum temperature rise shifts from the central oil film layer to the surface of solid b, which has a smaller rolling speed compared with the surface of solid a.

As a comparison, the sign of the sliding velocity is changed by making the rolling velocity of the surface of solid b larger than that of the surface of solid a, i.e., $u_b > u_a$, while the rolling speed of the contact u_r is kept constant, and results are shown in Fig. 4. As can be seen, the location of the maximum temperature rise shifts from the central oil film layer to the surface of solid a,

Downloaded From: https://heattransfer.asmedigitalcollection.asme.org/pdfaccess.ashx?url=/data/journals/jhtrao/936122/ on 04/16/2017 Terms of Use: http://www.asme.org/abou

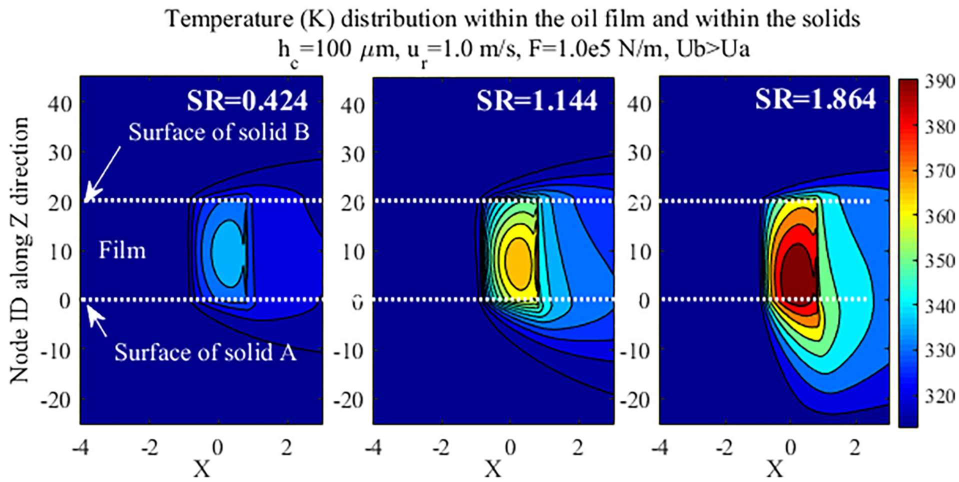

Fig. 4 The temperature distribution under three slide-to-roll ratio cases with $u_b > u_a$

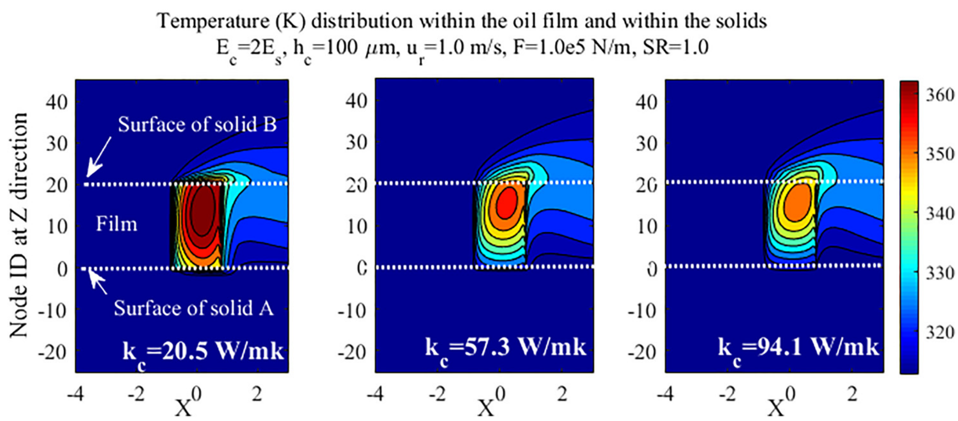

Fig. 5 Temperature distribution under three thermal conductivities of the coating

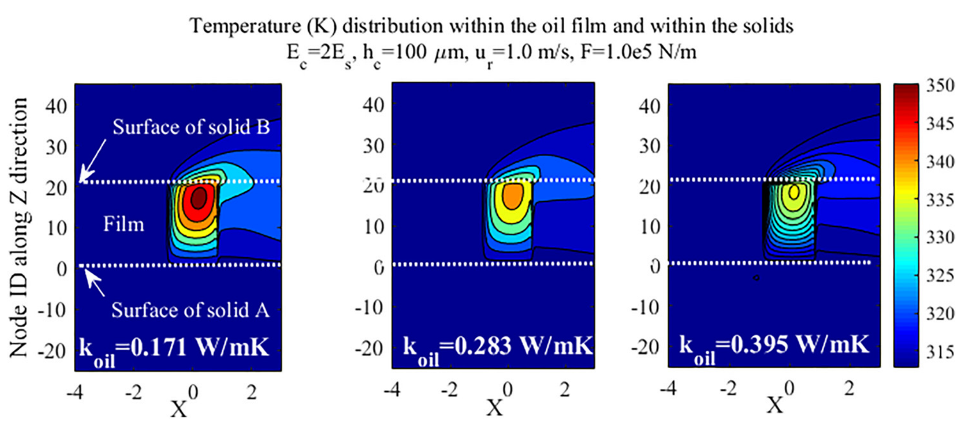

Fig. 6 Effect of the thermal conductivity of the fluid on temperature distribution

which has a smaller rolling speed. And this tendency becomes more clear as the slide-to-roll ratio increases.

Thermal conductivity is an important property for heat transfer. The thermal conductivity of a material represents the ability to transfer heat by conduction. Reference [21] defines two thermal conductivities $k_c = 5\,\mathrm{W/m\,K}$ and $k_c = 90\,\mathrm{W/m\,K}$ to investigate the effect of the thermal inertia. Figure 5 shows the detailed temperature distribution under three thermal conductivities of the coating, ranging from $k_c = 2.1\,\mathrm{W/m\,K}$ to $k_c = 186.1\,\mathrm{W/m\,K}$. The maximum temperature rise decreases from 360 K to 345 K, when the thermal conductivity of the coating increases from $k_c = 2.1\,\mathrm{W/m\,K}$ to $k_c = 186.1\,\mathrm{W/m\,K}$. The coating with a relatively low thermal conductivity prevents heat generated by the oil film shear action from being diffused from the center of the contact toward the peripheral area and the solids, which would lead to a high temperature rise within the center of the contact.

Effect of thermal conductivity of the oil is shown in Fig. 6 with three cases: $k_{\mathrm{oil}} = 0.171,\ 0.283,\ 0.395\,\mathrm{W/m\,K}$. As the thermal conductivity of the oil increases from $k_{\mathrm{oil}} = 0.171\,\mathrm{W/m\,K}$ to $k_{\mathrm{oil}} = 0.395\,\mathrm{W/m\,K}$, the maximum temperature rise within the contact area decreases from 350 K to 335 K. The temperature rise mainly occurs at the center of the Hertzian contact region, and the

Downloaded From: https://heattransfer.asmedigitalcollection.asme.org/pdfaccess.ashx?url=/data/journals/jhtrao/936122/ on 04/16/2017 Terms of Use: http://www.asme.org/abou

temperature within the oil film is much higher than that within the solids. The high ability of the oil to conduct heat assists the heat diffusing to the peripheral area and the solids, which further leads to the reduction of the temperature within the oil film. The increase of the thermal conductivity of the coating and of the oil film is helpful for the restraint of the temperature rise during contact.

Conclusion

Effect of the thermal properties of a coated EHL line contact is studied by emphasizing the difference between the thermal properties of the coating and of the substrate. Heat continuity conditions are satisfied at the surfaces of the solids and the coating/substrate interfaces. The maximum temperature rise increases from 5% for the case with slide-to-roll ratio $\mathrm{SR} = 0.424$ to 21% for the case with $\mathrm{SR} = 1.864$. The direction of the sliding velocity causes the difference in temperature between the two surfaces of solids. The temperature of the surface with the smaller rolling velocity is higher than that of the surface with the larger rolling velocity. The maximum temperature rise decreases from 360 K to 345 K when the thermal conductivity of the coating increases from $k_c = 2.1\,\mathrm{W/m\,K}$ to $k_c = 186.1\,\mathrm{W/m\,K}$. The coating with a relatively low thermal conductivity prevents heat generated by the oil film shear action from being diffused from the center of the contact toward the peripheral area and the solids, which would lead to a high temperature rise within the center of the contact. As the thermal conductivity of the oil increases from $k_{\mathrm{oil}} = 0.171\,\mathrm{W/m\,K}$ to $k_{\mathrm{oil}} = 0.395\,\mathrm{W/m\,K}$, the maximum temperature rise within the contact area decreases from 350 K to 335 K.

Acknowledgment

This work is financially supported by the National Natural Science Foundation of China (Grant Nos. 51405042, 51535012, and 51575061) and the China Postdoctoral Science Foundation (Grant No. 2015M582516).

Nomenclature

b_h = the Hertzian contact half-width under the uncoated case, m
c_c = heat capacity of the coating material, J/kg K
c_s = heat capacity of the substrate material, J/kg K
c_{oil} = heat capacity of the oil, J/kg K
d = the depth at the bottom boundary of the calculational domain, m
E_c = Young's modulus of the coating, Pa
E_s = Young's modulus of the substrate, Pa
F = the normal load, N
h_{ca}, h_{cb} = coating thickness of the two solids a and b, respectively, m
I = all variables should appear in italics
k_c = thermal conductivity of the coating material, W/m K
k_s = thermal conductivity of the substrate material, W/m K
k_{oil} = thermal conductivity of the oil, W/m K
p = the contact pressure, Pa
R_a, R_b = radius of curvature of the two solids a and b, respectively, m
SR = the slide-to-roll ratio
T_0 = ambient temperature and the inlet oil temperature, K
u_r = the rolling speed, m/s
ν = the Poisson's ratio of materials
α = the pressure–viscosity coefficient, Pa^{-1}
η_{oil} = the current oil viscosity, $\mathrm{Pa \cdot s}$
η_{oil0} = oil viscosity at ambient pressure, $\mathrm{Pa \cdot s}$
ρ_c = the density of the coating material, $\mathrm{kg/m^3}$
ρ_s = the density of the substrate material, $\mathrm{kg/m^3}$
ρ_{oil} = the density of the oil, $\mathrm{kg/m^3}$
ρ_{oil0} = the ambient density of the oil, $\mathrm{kg/m^3}$
τ_0 = the Eyring characteristic stress, Pa

References

[1] Alanou, M. P., Snidle, R. W., Evans, H. P., and Krantz, T. L., 2002, "On the Performance of Thin Hard Coatings for Gearing Applications," Tribol. Trans., **45**(3), pp. 334–344.
[2] Vera, E. E., Vite, M., Gallardo, E. A., and Laguna-Camacho, J. R., 2013, "Fatigue Life of TiN and CrN Coatings in Rolling Contact," Proc. Inst. Mech. Eng., Part J, **227**(4), pp. 339–348.
[3] Dearnley, P. A., Elwafi, A. M., Chittenden, R. J., and Barton, D. C., 2014, "Wear and Friction of Diamondlike-Carbon Coated and Uncoated Steel Roller Bearings Under High Contact Pressure Oil Lubricated Rolling/Sliding Conditions," ASME J. Tribol., **136**(2), p. 021101.
[4] Kano, M., 2006, "Super Low Friction of DLC Applied to Engine Cam Follower Lubricated With Ester-Containing Oil," Tribol. Int., **39**(12), pp. 1682–1685.
[5] Elsharkawy, A. A., and Hamrock, B. J., 1993, "A Numerical Solution for Dry Sliding Line Contact of Multi-Layered Elastic Bodies," ASME J. Tribol., **115**(2), pp. 237–245.
[6] Jin, Z. M., 2000, "Elastohydrodynamic Lubrication of a Circular Point Contact for a Compliant Layered Surface Bonded to a Rigid Substrate—Part 1: Theoretical Formulation and Numerical Method," Proc. Inst. Mech. Eng., Part J, **214**(3), pp. 267–279.
[7] Wang, Z. J., Yu, C. J., and Wang, Q., 2015, "Model for Elastohydrodynamic Lubrication of Multilayered Materials," ASME J. Tribol., **137**(1), p. 011501.
[8] Liu, H., Zhu, C., Wang, Z., Zhou, Y., and Zhang, Y., 2016, "A Theoretical Tribological Comparison Between Soft and Hard Coatings of Spur Gear Pairs," ASME J. Tribol., (accepted).
[9] Björling, M., Isaksson, P., Marklund, P., and Larsson, R., 2012, "The Influence of DLC Coating on EHL Friction Coefficient," Tribol. Lett., **47**(2), pp. 285–294.
[10] Yang, P., Qu, S., Kaneta, M., and Nishikawa, H., 2001, "Formation of Steady Dimples in Point TEHL Contacts," ASME J. Tribol., **123**(1), pp. 42–49.
[11] Liu, Y., Erdemir, A., and Meletis, E. I., 1996, "A Study of the Wear Mechanism of Diamond-Like Carbon Films," Surf. Coat. Technol., **82**(1–2), pp. 48–56.
[12] Yang, P., and Wen, S., 1990, "A Generalized Reynolds Equation for Non-Newtonian Thermal Elastohydrodynamic Lubrication," ASME J. Tribol., **112**(4), pp. 631–636.
[13] Liu, Y., 2013, "EHL of Coated Bodies," *Encyclopedia of Tribology*, Springer, New York, pp. 847–852.
[14] Liu, S., Wang, Q., and Liu, G., 2000, "A Versatile Method of Discrete Convolution and FFT (DC-FFT) for Contact Analyses," Wear, **243**(1–2), pp. 101–111.
[15] Liu, H., 2013, "Lubricated Contact Analysis of a Spur Gear Pair With Dynamic Loads," Ph.D. thesis, School of Engineering, University of Warwick, Coventry, UK.
[16] Yang, P., 1998, *Numerical Analysis of Fluid Lubrication*, National Defence Industry Press, Beijing, China.
[17] Liu, H., Zhu, C., Sun, Z., and Song, C., 2016, "Starved Lubrication of a Spur Gear Pair," Tribol. Int., **94**, pp. 52–60.
[18] Liu, S., Peyronnel, A., Wang, Q. J., and Keer, L. M., 2005, "An Extension of the Hertz Theory for 2D Coated Components," Tribol. Lett., **18**(4), pp. 505–511.
[19] Houpert, L., 1985, "New Results of Traction Force Calculations in Elastohydrodynamic Contacts," ASME J. Tribol., **107**(2), pp. 241–245.
[20] Dowson, D., and Higginson, G., 1966, *Elastohydrodynamic Lubrication*, Pergamon Press, Oxford, UK.
[21] Habchi, W., 2014, "A Numerical Model for the Solution of Thermal Elastohydrodynamic Lubrication in Coated Circular Contacts," Tribol. Int., **73**, pp. 57–68.
[22] Wang, Z. J., Wang, W. Z., Wang, H., and Hu, Y. Z., 2009, "Stress Analysis on Layered Materials in Point Elastohydrodynamic-Lubricated Contacts," Tribol. Lett., **35**(3), pp. 229–244.
[23] King, R. B., and O'Sullivan, T. C., 1987, "Sliding Contact Stresses in a Two-Dimensional Layered Elastic Half-Space," Int. J. Solids Struct., **23**(5), pp. 581–597.

Downloaded From: https://heattransfer.asmedigitalcollection.asme.org/pdfaccess.ashx?url=/data/journals/jhtrao/936122/ on 04/16/2017 Terms of Use: http://www.asme.org/abou